Traffic Sign Detection and Classification using Colour and Shape Cues

F.P. Senekal

Council for Scientific and Industrial Research, South Africa

fsenekal@csir.co.za

Abstract

This paper presents a new technique for the recognition of road traffic signs. The technique is based on colour and shape analysis of a single image. It is aimed at the detection and classification of triangular traffic signs, such as warning and yield signs. The technique is applied to a set of images obtained from a camera mounted on a moving vehicle. Good detection and classification performance is achieved.

1. Introduction

The ability to recognise road and traffic signs is becoming an important research area in *Intelligent Transport Systems* (ITS) and has a number of applications. In *driver support systems*, such a system could focus a driver's attention to road conditions ahead, such as pedestrians that may be crossing the road or a change in the allowed speed limit, allowing the driver to take appropriate action on time. In *intelligent autonomous vehicles*, the ability to recognise and interpret such signs could contribute greatly to their control and safe navigation. For example, a sign indicating that there is a stop ahead may lead the control system to reduce the speed of the vehicle. In *highway maintenance* and *sign inventory* applications, the ability to recognise and possibly to evaluate the condition of the signs, can greatly reduce the effort in maintaining current road infrastructure.

Traffic signs are designed to have specific saturated colours that are easily distinguishable from their environment. In South Africa and many other countries, typical control, prohibition and warning signs contain red, black and/or white; typical command and reservation signs contain blue and/or white; and typical route markers and tourism signs contain green, blue or brown with white and/or yellow lettering. They also have specific shapes; command and prohibition signs are circular, warning signs and yield signs are triangular, reservation, route markers and tourism signs are rectangular and stop signs are octagonal. They are placed near the road surface in a clearly visible position, usually free from any occlusions. Figure 1 shows examples of commonly occuring traffic signs.

Figure 1: *Typical traffic signs, showing their unique colour and shape (from left to right: stop, yield, pedestrians only, 100km/h speed limit, no u-turn, pedestrian crossing ahead) (note that images are available in colour).*

The fact that traffic signs have unique colours and shapes are often exploited in algorithms designed to recognise them. These algorithms typically follow a two step process. In the *detection* phase, the position and shape of the signs (if any) in the image are determined. In the *classification* phase, the aim is to assign class labels to the signs that were detected. Detection and classification usually constitute recognition in the scientific literature. A third *applicability* phase may be required to determine whether a given sign in the visual field is applicable in the current situation or, put differently, to recognise whether a particular sign is relevant in the current context of the application. This is particularly important in applications such as driver support systems and intelligent autonomous vehicles. Although robust detection and classification algorithms have been developed, determining the applicability of a sign is a difficult task that has not been adequately addressed in the literature and presents an opportunity for future research.

Detection is usually performed on colour images, although some studies have also been executed on grayscale images. When colour images are used, segmentation through colour thresholding, region detection and shape analysis are usually performed. The choice of colour space is important during the detection phase. When the RGB colour space is used [1, 2, 3], thresholding is usually based on relations between the colour components. Others work in the HSI or HSV colour space [4, 5, 6], where the relations between the components is somewhat simplified. Other colour spaces, such as LUV [8] and CIECAM [9] have also been used. Due to the varying colour conditions that may occur, more extensive approaches have also been developed. Databases for colour pixel classification are used in [10] and [11]. Fuzzy classification [12] and neural networks [13] have also been tried. Border detection on grayscale images [14] is another approach that have been taken.

Classification can be accomplished by a number of approaches. Template matching is used in [15] and [16]. Multilayer perceptrons [1, 17], radial basis function networks [18], Laplace kernel classifiers [19] and genetic algorithms [4] have also been studied.

The recognition of traffic signs presents a number of difficulties, both in terms of the *image formation process* and in terms of the *environment* in which the sign is found. In the image formation process, the size of the sign in the image depends on its physical size and its distance from the camera and in general could be arbitrarily rotated. There will be an aspect modification in the projection of the sign in the image if the optical axis of the camera is not perpendicular to the sign (i.e. perspective distortion). There is also no standard colour associated with the signs, as the colour will depend on various photometric effects. In addition, effects such as sensor noise and motion blur may be present in the image. Difficulties in the environment in which the sign is found can be divided into four groups, illustrated in Figure 2. The *physical condition* of the sign may make recognition difficult, such as the effect of deteriorating paint quality over time (Fig. 2a), signs that are damaged (Fig. 2b), signs that are incorrectly placed, the presence of graffiti

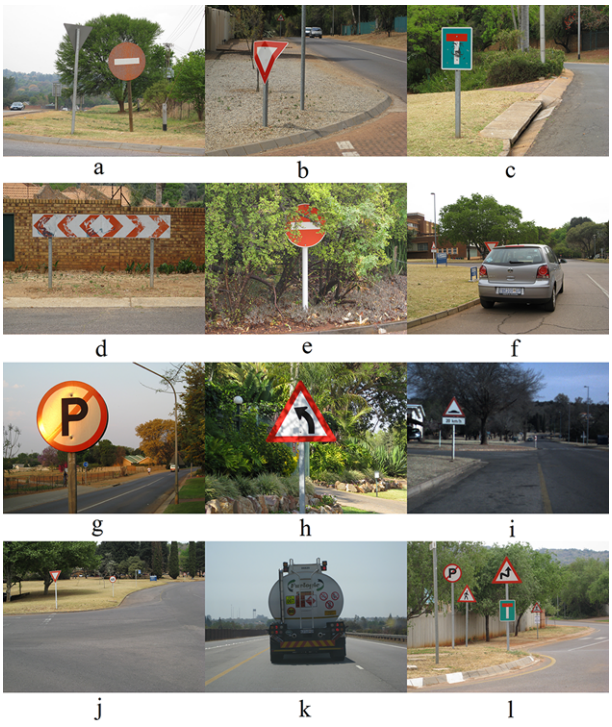

Figure 2: *Difficulties in the recognition of traffic signs: (a) deteriorating paint quality, (b) damaged sign, (c) graffiti, (d) general deterioration, (e) partial occlusion by a static object, (g) partial occlusion by a dynamic object, (g) reflections, (h) shadows, (i) low-light conditions, (j) sign not applicable, (k) sign not applicable, (l) too many signs.*

(Fig. 2c) or just general deterioration of the sign (Fig. 2d). *Partial occlusions* of the sign, both of a static (Fig. 2e) and dynamic (Fig. 2f) nature, and *lighting conditions* such as reflections (Fig. 2g), shadows (Fig. 2h) and low-light conditions (Fig. 2i) may also have a severe influence. Finally, there may be difficulty in determining the *applicability* of a traffic sign. In Fig. 2j the yield sign is only applicable to drivers using the side road, in Fig. 2k the speed sign is applicable only to the vehicle with which it is associated and in Fig. 2l there may be general confusion due to the many signs present.

2. Method

In the work presented here, the interest is in recognising *triangular signs* such as warning and yield signs. These signs have a red triangular frame that usually surrounds a black iconic representation of an object on a white background. The algorithm discussed here can be applied to a single image, i.e. it is not dependent on temporal consistencies between successive frames in a video sequence. It is assumed that the traffic sign is not occluded by objects in the environment in such a way as to segment its projection onto the image plane into different regions or in such a way that the visible portion of the interior of the sign is fundamentally altered. A further assumption is that the sign is fully contained in the interior of the image, i.e. it does not protrude beyond the boundaries of the image.

An overview of the steps in the algorithm is shown in Figure 3. An example of the output of some of these steps is shown in Figure 4, using the source image shown in Fig. 4a. The steps

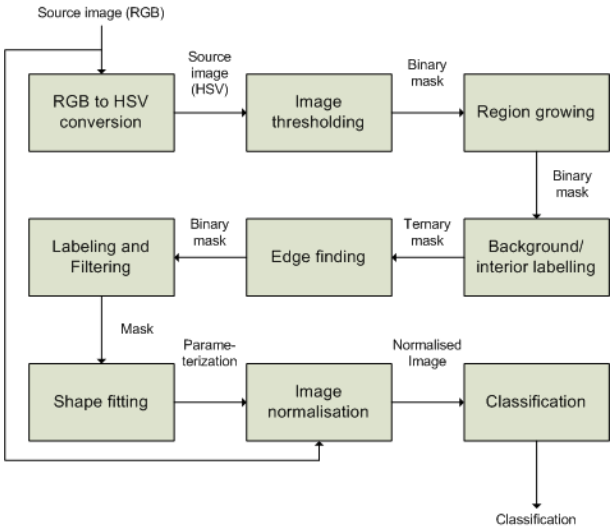

Figure 3: *Steps in the recognition of traffic signs.*

are discussed in detail in the subsections that follow; here a brief overview is given.

The image is converted from the RGB to the HSV colour space, after which an initial threshold is applied to determine red regions (possible traffic signs) (Fig. 4b - background shown as white). These red regions are "grown" to include other possible regions that may qualify but which may not have qualified during the initial thresholding step. Next, the interiors and exteriors (background) of possible signs are marked (Fig. 4c - background in white, interiors in yellow). This process is likely to fail in the presence of occlusions, where the interior and exterior regions are connected and thus not be easily separable. Edges are then extracted from the image where the interiors touch the possible signs (Fig. 4d). A component labelling algorithm is then applied to determine different edge segments that are 8-connected. Small edge segments that are likely to be noise is discarded (Fig. 4e). Separate edge segments are tested to determine whether they provide a good fit for a triangle (Fig. 4f). If such a fit is established, the three vertices of the triangle are noted. Using these vertices, interpolation based on barycentric coordinates is applied to map the triangle in the original image onto a new normalised triangle with fixed scale and rotation (Fig. 4g). This normalisation also aims to reduce the effect of perspective distortion. Classification is achieved by matching this normalised triangle to a set of reference templates.

2.1. Colour Conversion

Most digital image formats store a digital image as a series of two-dimensional arrays, specifying the red, green and blue (RGB) channels. The first step is to convert each pixel of the source image to its equivalent in the hue, saturation and value (HSV) colour space. The HSV colour space provides a convenient interpretation of the meaning of colour. The reader is referred to [22, p.623] for a description of the conversion process.

2.2. Image Thresholding

The fact that triangular signs have a characteristic red frame can be exploited to identify regions in the image that could possibly contain such signs. The image is thresholded to identify regions

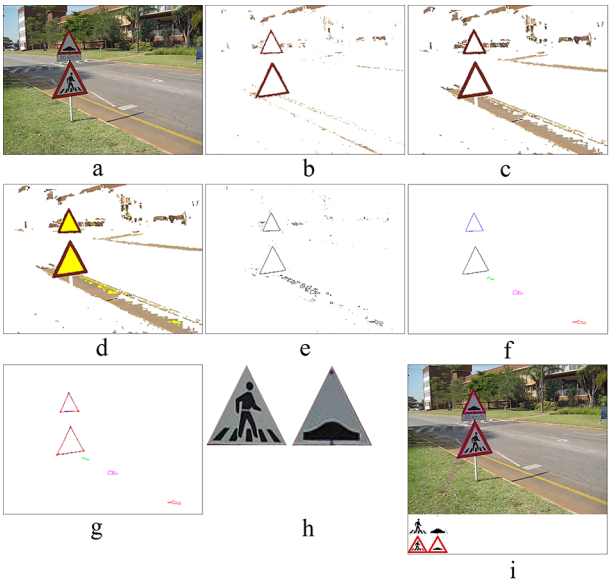

Figure 4: *Output of the various steps in the recognition process: (a) source image, (b) after thresholding, (c) after background/interior labelling, (d) after edge finding, (e) after labelling and filtering, (f) after shape fitting, (g) after normalised images have been extracted, (h) after classification.*

with red pixels. The output of this process is a mask that specifies for every pixel whether it is adequately red or not.

The hue and saturation components are sufficient in identifying red regions in warning signs. The mask is defined as

$$\mu_1(x,y) = \begin{cases} 1, & \text{if } S(x,y) \geq T_S \text{ and} \\ & (H(x,y) \leq T_H \text{ or } H(x,y) \geq 1 - T_H), \\ 0, & \text{otherwise,} \end{cases} \tag{1}$$

where T_S is a threshold related to the saturation of the pixel, and T_H is a threshold related to the hue of the pixel and S and H are the saturation and hue respectively at coordinate (x, y).

Since hue values close to 0 and 1 are indicative or red, there are two conditions related to the hue value. The output of this step is shown in Figure 4b (object pixels are shown in their original colour, background pixels are white).

2.3. Region Growing

For a variety of reasons, such as a sign's paint that fade over time or the presence of reflections and shadows, the frame of the sign may contain regions that are not a highly saturated red colour. Such regions may not be detected under the mask defined by (1).

Under the assumption that such regions will be close to the regions identified by (1), and that they will be "somewhat" red, the mask can be grown to include such regions. The new red mask μ_2 is expressed by

$$\mu_2(x,y) = \begin{cases} 1, & \text{if } \mu_1(x,y) = 1 \text{ or} \\ & (S(x,y) \geq t_S \text{ and} \\ & (H(x,y) \leq t_H \text{ or } H(x,y) \geq 1 - t_H) \text{ and} \\ & \exists (x_0,y_0) \in N(x,y) \text{ s.t. } \mu_1(x_0,y_0) = 1), \\ 0, & \text{otherwise,} \end{cases} \tag{2}$$

where t_S and t_H are new threshold values and $N(x, y)$ is a neighbourhood of (x, y). Note that proximity to a pixel that is already classified as red is required, but the thresholding conditions are relaxed such that $t_S \leq T_S$ and $t_H \geq T_H$. The procedure can be applied iteratively, replacing the previous mask by the new mask, and can be stopped after convergence.

2.4. Background/Interior Labelling

At this stage, it is undecided whether a given non-object pixel (corresponding to a 0 in the mask) is internal or external (background) to the object.

As was previously mentioned, the assumption is made that the sign is fully contained in the interior of the image (we are not making predictions about signs that protrude across the boundaries of the image). Under this assumption, all internal pixels are completely surrounded by at least a single line of object pixels. No internal pixels are thus found in the boundary (the first and last rows and columns) of the image.

We can exploit this assumption by noting where mask boundary that have a value of 0 and correspondingly marking them as background. Using these coordinates as seed values, we recursively find 4-connected pixel neighbours, and each such neighbour which also has a mask value of 0 is then also marked as background. After the recursion process, all coordinates with a mask that has a value of 0 and which has not been marked as background are interior pixels. It is possible for remaining values not to be "true" interiors but rather to exist due to the boundaries of the objects surrounding them touching each other. However, such regions will be completely surrounded by the object boundaries and thus cannot be distinguished from true interiors.

Mathematically, this can be expressed as

$$\mu_3(x,y) = \begin{cases} 1, & \text{if } \mu_2(x,y) = 1, \\ -1, & \text{if } \exists (x_0,y_0) \in B \text{ s.t. there exists} \\ & \text{a 4-connected path } P \text{ between } (x,y) \text{ and} \\ & (x_0,y_0) \text{ s.t. } \mu_2(x_i,y_i) = 0 \forall (x_i,y_i) \in P, \\ 0, & \text{otherwise,} \end{cases} \tag{3}$$

where B is the set of pixel coordinates defining the boundary of the image, P is a set of pixel coordinates defining a 4-connected path between $(x0, y0)$ and (x, y)..

The output of this step is shown in Figure 4c, where yellow is used to indicates an internal pixel and white a background pixel. Object pixels are shown in their original colours.

2.5. Edge Finding

The next step in the algorithm is to find the pixels corresponding to the object-interior edges. An edge in this context is defined as any interior pixel that is 4-connected to an object pixel, and is given by

$$\mu_4(x,y) = \begin{cases} 1, & \text{if } \mu_3(x,y) = 0 \text{ and} \\ & (\mu_3(x+1,y) = 1 \text{ or } \mu_3(x-1,y) = 1 \text{ or} \\ & \mu_3(x,y+1) = 1 \text{ or } \mu_3(x,y-1) = 1), \\ 0, & \text{otherwise.} \end{cases} \tag{4}$$

The output of this step is shown in Figure 4d, where a black indicates an edge and a white a non-edge.

2.6. Labelling and Filtering

A connected component labelling algorithm is applied to the mask to determine which edges are 8-connected. A two-pass algorithm is applied. In the first pass, an initial labelling of

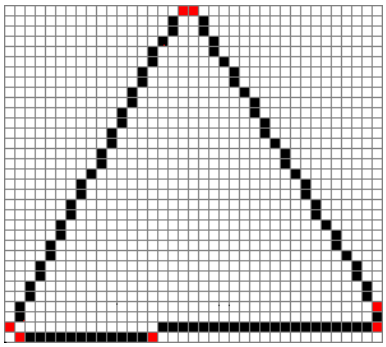

Figure 5: *Connection points (indicated in red) used for line fitting.*

the edges in single scan lines is performed. Labelling conflicts between successive scan lines are noted. On completion of the first pass, the union find algorithm [20, pp. 441-440] is applied to resolve labelling conflicts. A second pass is performed to re-label each of the original edge labels.

The labelling algorithm produces a new mask μ_5. A positive value of $i = \mu_5(x, y)$ indicates that the coordinate (x, y) is associated with the *i*'th edge object.

The area of each edge object is calculated as

$$A_i = \sum_{\mu_5} a_i, \text{ where } a_i = \begin{cases} 1, & \text{if } \mu_5(x,y) = i, \\ 0, & \text{otherwise,} \end{cases} \quad (5)$$

where the sum is taken over all image coordinates (x, y). Edge objects with a large enough areas are retained, that is edge objects for which $A_i \geq T_A$, where T_A is a threshold specifying the minimum area. The step is likely to filter out edge objects that are present due to noise. In addition, edge objects that correspond to small areas for which a classification would in any case not be possible are filtered out.

The output of this step is shown in Figure 4e, where different colours are used to represent the different edge objects that are retained.

2.7. Shape Fitting

The previous step will retain all edge objects that have a large enough area to merit further consideration. In this step, the objective is to determine whether these edge objects provide a good fit to a triangle. The approach taken is to fit various lines through edge pixels. An algorithm such as RANSAC could be applied for this purpose, but a deterministic approach is sought for robust detection.

This is achieved by means of "connection points" (illustrated in Figure 5). Given the bounding box of the edge object, the connection points are defined as the most top-left, top-right, right-top, right-bottom, bottom-right, bottom-left, left-bottom and left-top pixel coordinates in the bounding box that form part of the edge object. Connection points with the same coordinates are noted as a single point. There are thus a maximum of 8 unique connection points. Let N be the number of such unique points.

A line segment is fitted through successive pairs of successive connection points (modulo N), using their coordinates as beginning and end points for the line segment. For each such line segment, the closest distance d from each edge object coordinate to the line segment is calculated. All edge object coordinates within a distance $d \leq D$ are noted. Let the number of such points be S_i (i varies from 1 to N). This represents a score associated with the line segment i. For each line segment, a linear least squares approximation is performed to determine the equation of a line that fits through the S_i points.

The N lines are now sorted according to the score S_i associated with each line, in descending order. Some of these lines may be associated with the same side of a triangle and thus need to be filtered out. To achieve this, a new list of lines is created. Working in descending order of score, a line is added to the new list if it has a non-overlapping angle with any of the lines already in the list. Two lines are overlapping if their angular difference is less than a threshold T_θ. The three top scoring, non-overlapping lines are used for triangle estimation. If there are less than three such lines, the detection process is stopped.

The sum of the scores associated with these three lines is noted (filtering out coordinates that contribute more than once in each of the individual scores). Let the sum of these scores be S. For a good fit, it is required that $S \geq k_S A_i$, for some $0 \leq k_S \leq 1$. If such a good fit exists, the intersection points of the three lines are determined. Let these points be $P_i = (x_i, y_i), i = 1, 2, 3$. A final test is performed to determine whether these intersection points are within a certain distance from the bounding box of the edge segment and within the bounds of the image. If this is the case, it is assumed that a triangle is successfully detected.

A distinction is made between the "yield" (pointing to the bottom) and "warning" (pointing to the top) configuration of the triangle. Let y_{min} represent the minimum of the three triangle y-coordinates and y_{max} the maximum. The yield configuration is assumed if two of the y-coordinates of the triangle are less than $\frac{ymin+ymax}{2}$ and the warning configuration is assumed otherwise. The coordinates P_i defining the triangle are reordered. In the case of the yield configuration the order is top-left, top-right, bottom-centre and in the case of the warning configuration the order is top-centre, bottom-left, bottom-right.

The output of this step is shown in Figure 4f, where the detected triangle sides are indicated in red.

2.8. Image Normalisation

A normalised image with dimensions $L \times L$ pixels is now created. A useful choice, if multiresolution techniques is to be applied, is to let L be of the form 2^n. In the case of the yield configuration, the coordinates defining the normalised triangle is given by p_1 = (0, 0), p_2 = (0, L-1) and p_3 = ($\frac{L-1}{2}$, L-1) and in the case of the warning configuration, these coordinates are p_1 = (0, $\frac{L-1}{2}$), p_2 = (L-1, 0) and p_3 = (L-1, L-1). A mapping is required that will map the triangle defined by the coordinates P_i in the original image to a triangle defined by the coordinates p_i in the normalised image.

To achieve this, barycentric coordinates are used. A point $p = (x, y)$ within the bounds of the triangle defined by the p_i coordinates is expressed as $p = w_1 p_1 + w_2 p_2 + w_3 p_3$, where w_i are weights such that $w_1 + w_2 + w_3 = 1$. $[w_1, w_2, w_3]$ are the barycentric coordinates. For a warning configuration, the coordinates are given by

$$w_1 = \frac{-1}{L-1} y + 1 \quad (6)$$

$$w_2 = \frac{-1}{L-1} x + \frac{1}{2(L-1)} y + \frac{1}{2} \quad (7)$$

$$w_3 = 1 - w_1 - w_2, \quad (8)$$

and for the yield configuration, the coordinates are given by

$$w_3 = \frac{1}{L-1}y \tag{9}$$

$$w_2 = \frac{1}{L-1}x - \frac{1}{2(L-1)}y \tag{10}$$

$$w_1 = 1 - w_2 - w_3. \tag{11}$$

The barycentric coordinates are calculated for each pixel in the normalised image that lies within the triangle. A corresponding point P in the original image is then calculated as $P = w_1P_1 + w_2P_2 + w_3P_3$. Using this coordinate, bilinear interpolation is applied to determine a red, green and blue value for the pixel in the normalised image.

2.9. Classification

A grayscale version of the normalised image is calculated. The classification approaches taken for warning and yield signs are slightly different. For warning signs a binary image is created from the grayscale image through thresholding. Due to the possible variety of lighting conditions, a single threshold value will not be sufficient in all cases. To address this, a dynamic thresholding algorithm as described in [22, pp. 599-600] is implemented. The histogram of the grayscale values is calculated. The objective is to find a threshold value that will clearly distinguish between dark and light regions in the image, which is akin to finding a "good" separation between the two peaks in the histogram. The median grayscale value is chosen as the initial threshold. Two means are calculated: the mean of pixels darker than the threshold and the mean of pixels lighter than the threshold. The average of the two means is taken as the next threshold value. Threshold values are iteratively calculated until convergence is achieved.

Let $b(x, y)$ represent the resulting binary image with dimensions $L \times L$. The geometric mean of the binary image is calculated as

$$(m_x, m_y) = \frac{1}{N_b}(\sum_{x=0}^{L-1}\sum_{y=0}^{L-1}(1-b(x,y))x, \sum_{x=0}^{L-1}\sum_{y=0}^{L-1}(1-b(x,y))y), \tag{12}$$

where the values 0 and 1 in the binary image represent black and white respectively and N_b is the number of black pixels.

The binary image is compared to a set of reference templates. This is achieved by aligning the binary image with each reference template by their mean coordinates and calculating the number of pixel differences δ_i in the intersection of the binary image with the i^{th} reference image. Let δ_{min} be the minimum over all δ_i and I the index associated with the minimum. The sign is classified as belonging to class I if $\delta_{min} \leq T_\delta$, where T_δ is a threshold specifying the maximum allowed difference between the image and the template. If the minimum distance is larger than the threshold, no classification is made.

For yield signs the approach taken is different. Since the proper yield sign consists only of light pixels, a dynamic thresholding technique would fail, thus necessitating a different technique. The Euclidean distance between the grayscale image and the template image is calculated and the class associated with the minimum distance is assigned. Since there are only two types of yield signs, this approach works well.

3. Results and Discussion

To create the template images, reference sheets of the official traffic sign designs were obtained from the Department of Transport in South Africa [21]. From these sheets, the templates for 87 warning signs (which is further subdivided into road layout signs, direction of movement signs and symbolic signs) and two yield signs were created.

The colour threshold parameters used were T_S = 0.75, T_H = 0.05, t_S = 0.5 and t_H = 0.1. The area threshold was set at T_A = 50 pixels. The neighbourhood operation in Equation 2 was taken to mean 8-connected pixels. For line fitting, D = 2 pixels, $T_\theta = 5$ degrees and k_S = 0.9 was used. Images were normalised to L = 256 pixels in the vertical and horizontal dimensions. No threshold was applied during classification, that is $T_\delta = \infty$.

The algorithm was tested on images extracted from a number of video sequences. The images were captured at a resolution of 640 x 480 pixels in RGB format and with 8 bits per channel. Video sequences 1 to 5 were captured under good daylight conditions, with the focus on a specific traffic sign(s) and with the sign occupying a relatively large area of the image (from 26 to 235 pixels in the horizontal dimension). Video sequences 6 to 8 were captured from a moving vehicle, with the camera pointed forward in the direction of the vehicle movement, so that different signs are present in the video. These videos present a greater challenge, since the signs are relatively small (from 20 to 60 pixels in the horizontal dimension) and the camera is not always focussed on them.

The results obtained by applying the algorithm are shown in Table 1. Classification was attempted only on signs where a true positive detection was made. To describe the results of the detection and classification processes in a meaningful way, the positive predictive value (PPV) was defined as $PPV = \frac{C}{TPD+FPD}$ and the sensitivity as $SN = \frac{C}{TPD+FND}$. Note that a classification is attempted for each detection ($T_\delta = \infty$). the PPV and sensitivity values may be improved by rejecting detections for which there is a low confidence in correct classification.

As may be expected, the PPV and sensitivity are significantly better for video sequences 1 to 5 than for sequences 6 to 8. An analysis of the images for which errors occurs reveals that false negatives are mainly the result of the signs having a darkish red colour that is not detected through the thresholding process. Noise on the object-interior boundary also result in detection failures. False positives are mainly the result of areas in the background (such as ground or buildings) that masquerade as reddish areas that surround a triangular interior. Classification errors are typically the result of a weak triangular fit that rotates the normalised image.

Table 1: *Summary of the results obtained using the algorithm described in this paper (legend: PR - (horizontal) pixel range, #S - number of signs, TPD - true positive detections, FPD - false positive detections, FND - false negative detections, C - correct classifications, PPV - positive predictive value, SN - sensitivity).*

No	PR	#S	TPD	FPD	FND	C	PPV	SN
1	53-137	640	635	4	5	635	99.4	99.2
2	26-124	484	484	2	0	483	99.4	99.8
3	192-235	244	244	4	0	244	98.4	100
4	61-107	354	354	13	0	354	96.5	100
5	107-204	198	198	9	0	198	95.7	100
6	20-60	95	68	1	27	59	85.5	62.1
7	20-55	115	104	2	11	94	88.7	81.7
8	21-57	102	93	0	9	84	90.3	82.4

4. Conclusions and Future Work

The paper presents a new algorithm for the detection and classification of triangular traffic signs such as warning and yield signs, using colour and shape cues. The algorithm offers robust recognition capabilities under normal daylight conditions in the absence of occlusions.

The algorithm can be extended to other classes of traffic signs, such as control, command and prohibition signs. The approach for these signs could be similar to the approach presented in this algorithm, except that additional colours are used in the threshold process and that other types of shapes (ellipses, octagons, etc.) need to be fitted. In the case of command and prohibition signs, an additional difficulty that needs to be addressed during the normalisation step is to produce a normalised image that is rotation invariant. A more difficult challenge is the recognition and interpretation of sign boards, where there is no standard template and each such sign needs to be interpreted individually for its content.

An important problem to address is the presence of occlusions. The approach presented here is applicable only in the case where occlusions do not intersect the object such that its interior and exterior are connected. One way to solve this problem is to search directly for object-interior boundaries. This could be accomplished by a metric that specifies the extent to which two adjacent pixels are red and white respectively (or other colours for the other classes of signs). These "fuzzy" edges could be thresholded and the algorithm could proceed with labelling and filtering, shape fitting, etc.

The work also needs to be extended to track a traffic sign across multiple frames in a video sequence.

5. Acknowledgments

The research conducted and reported on in this paper was funded by the Council for Scientific and Industrial Research (CSIR), South Africa, under the CSIR Autonomous Rover (CAR) project. The author would also like to thank Willie Brink for his suggestions during the development of the algorithm.

6. References

[1] A. de la Escalera, L. Moreno, M.A. Salichs and J.M. Armingol, "Road traffic sign detection and classification", *IEEE Transactions on Industrial Electronics*, Vol. 44, No. 6, pp. 848-859, 1997.

[2] S.K. Kim and D.A. Forsyth, "A new approach for road sign detection and recognition algorithm", 30th International Symposium on Automotive Technology and Automation, Robotics, Motion and Machine Vision in Automotive Industries, ISATA, 1997.

[3] M.M. Zadeh, T. Kasvand and C.Y. Suen, "Localization and recognition of traffic signs for automated vehicle control systems", *Intelligent Transportation Systems*, SPIE, 1998.

[4] A. de la Escalera, J.M. Armingol and M. Mata, "Traffic sign recognition and analysis for intelligent vehicles", *Image and Vision Computing*, Vol. 11, No. 3, pp. 247-258, 2003.

[5] P. Arnoul, M. Viala, J.P. Guerin and M. Mergy, "Traffic signs localisation for highways inventory from a video camera on board a moving collection van", Intelligent Vehicles Symposium, IEEE, 1996.

[6] T. Hibi, "Vision based extraction and recognition of road sign region from natural colour image, by using HSL and coordinates transformation", 29th International Symposium on Automotive Technology and Automation, Robotics, Motion and Machine Vision in the Automotive Industries, ISATA, 1996.

[7] H. Fleyeh and M. Dougherty, "Road and traffic sign detection and recognition", 10th EWGT Meeting and 16th Mini-EURO Conference, 2005.

[8] D.S. Kang, N.C. Grisworld and N. Kehtarnavaz, "An invariant traffic sign recognition system based on sequential color processing and geometrical transformation", Southwest Symposium on Image Analysis and Interpretation, IEEE, 2004.

[9] X. Gao, K. Hong, P. Passmore, L. Podladchikova and D. Shaposhnikov, "Colour vision model-based approach for segmentation of traffic signs", *EURASIP Journal on Image and Video Processing*, Vol. 2008.

[10] L. Priese, J. Klieber, R. Lakmann, V. Rehrmann and R. Schian, "New results on traffic sign recognition", Intelligent Vehicles Symposium, IEEE, 1994.

[11] L. Priese, R. Lakmann and V. Rehrmann, "Ideogram identification in a real-time traffic sign recognition system", Intelligent Vehicles Symposium, IEEE, 1995.

[12] G.Y. Jiang and T.Y. Choi, "Robust detection of landmarks in color image based on fuzzy set theory", Fourth International Conference on Signal Processing, IEEE, 1998.

[13] N. Bartneck and W. Ritter, "Colour segmentation with polynomial classification", 11th International Conference on Pattern Recognition, IAPR, 1992.

[14] H. Austerirmeier, U. Büker, B. Merstching and S. Zimmermann, "Analysis of traffic scenes using the hierarchical structure code", International Workshop on Structural and Syntactic Pattern Recognition, 1992.

[15] N. Barnes and A. Zelinsky, "Real-time radial symmetry for speed sign detection", In IEEE Intelligent Vehicles Syposium (IV), pp. 566-571, Parma, Italy, 2004.

[16] J. Miura, T. Kanda and Y. Shirai, "An active vision system for real-time traffic sign recognition", IN Proc. IEEE Conf. on Intelligent Transportation Systems, pp. 52-57, Dearborn, MI, 2000.

[17] J. Torresen, J.W. Bakke and L. Sekania, "Efficient recognition of speed limit signs", In Proc. IEEE Conf. on Intelligent Transportation Systems, Washington, DC, 2004.

[18] D.M. Gavrila, "Traffic sign recognition revisited", In Mustererkennung (DAGM), Bonn, Germany, 1999, Springer Verlag.

[19] P. Paclik, J. Novovicova, P. Somol and P. Pudil, "Road sign classification using Laplace kernel classifier", *Pattern Recognition Letters*, Vol. 21, pp. 1165-1173, 2000.

[20] R. Sedgewick, *Algorithms in C*, Addison-Wesley Publishing Company, Reading, Massachusetts, 1990.

[21] "Road and traffic information", $http://www.kzntransport.gov.za/rd\_traffic/enforcement/traffic\_signs/$, Last accessed 17 September 2008.

[22] R.C. Gonzalez and R.E. Woods, "Digital Image Processing", 2nd ed., Prentice Hall, New Jersey, 2002.